

Design of Gold Nanohole Arrays for Surface Plasmon Resonance Biosensing

Author: Marc Bernardo Ferré.

Advisor: Mauricio Moreno.

Facultat de Física, Universitat de Barcelona, Diagonal 645, 08028 Barcelona, Spain*.

Abstract: A study of the geometry effects of a SPR device based on a gold array of nanoholes has been done. Firstly, we obtained the dependence between the SPR peak position with the period, the hole's size and the thickness of the gold film. All this for two types of hole: circular and square shapes. Furthermore, we have simulated the effect of the refractive index of the medium on the reflection spectrum. Effectively, little changes in the refractive index provoke a shift in the SPR peak. It's the result we expected, because there are many devices based on calculating these changes on the medium through the reflection spectra obtained.

I. INTRODUCTION

The Surface Plasmon Resonance (SPR) is a phenomenon that occurs when a TM p-polarized light strikes on a metallic thin film covering a dielectric material, whose indexes have to satisfy the following conditions: $|\epsilon_2| > \epsilon_1$ and $|\epsilon_4| > \epsilon_5$. Some electrons in the metal start oscillating for a concrete angle producing a resonance effect, which implies an attenuation of the reflexed signal.

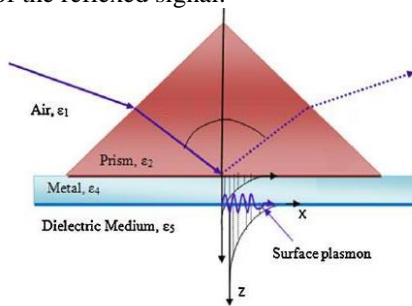


FIG. 1: When the incident light goes through the base of the prism, an evanescent field is produced, which induces another evanescent wave (coupling) in the other metal-dielectric surface. ¹

Another alternative to the angular device configuration (at fixed wavelength) is using the spectral mode (at fixed angle)⁶. Thus, we will have a reflective spectrum, where there is a narrow wavelength band that will produce the resonance, as it happens with the resonance angle. A decrease of the reflection will be detected as a consequence because the oscillation of the electrons in the resonance conditions for this wavelength.

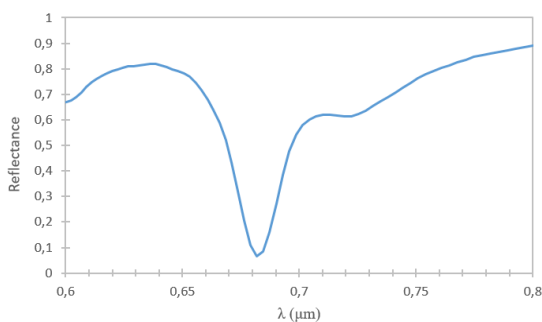


FIG. 2: Reflective spectrum calculated in our SPR simulation. We can see a decrease of the reflexion in a certain wavelength produced by the excitation of the plasma.

Instead of using a prism as the diffraction mechanism (FIG 1), it's possible to use a periodic structure. In our case, we will use a period array of nanoholes, where its function is to diffract the light. Varying the parameters of the hole, the dimensions of the gold layer, the refractive index of the medium, we can modify the resonance conditions affected by the plasmon absorption.

II. REAL APPLICATIONS

As we will see in the body of the work, depending on the refractive index (RI) of the external medium where the light travels, the peak in the reflection spectrum is shifted. Analysing that shift, we can determine really low variations of the surface refractive index, usually measured with RIUs (refractive index units). This little changes can be produced by a different concentration of molecules (analyte) bound to the immobilized ligand in the gold surface (see FIG. 3)².

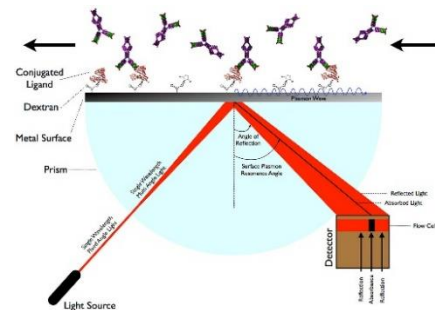


FIG. 3: Representation of a biosensor framework.

Until now, research has been focused on studying the reflection spectra, but there are more applications that can be made using this type of devices to take advantage of the special transmittance they have. Regulating accurately the position of the plasma absorption peaks, we can make optical filters of light, that they could filter some non-desirable wavelength of the incident spectrum.⁷

III. SOFTWARE USED

OptiFDTD³ is a powerful software that allows 3D designing and simulation of photonic components, as our SPR experiment is. The simulations are carried through the finite-difference time-domain (FDTD) method. It's a very useful method for simulating the light propagation, scattering, diffraction and polarization effect.

* Electronic address: befemarc@hotmail.com

The FDTD approach is based on a direct numerical solution of the time-dependent Maxwell curl equations:

$$\mu \frac{\partial \vec{H}}{\partial t} = -\nabla \times \vec{E} \quad (1)$$

$$\varepsilon \frac{\partial \vec{E}}{\partial t} + \sigma \vec{E} = \nabla \times \vec{H} \quad (2)$$

Considering the equation (1) and (2) and applying the second-order finite difference method, field notations and displacements, we can build the 3D-FDTD formulas which the domain is a cubic box where each field components is presented by a 3D array with E_x , E_y , E_z , H_x , H_y , H_z , as the following figure shows:

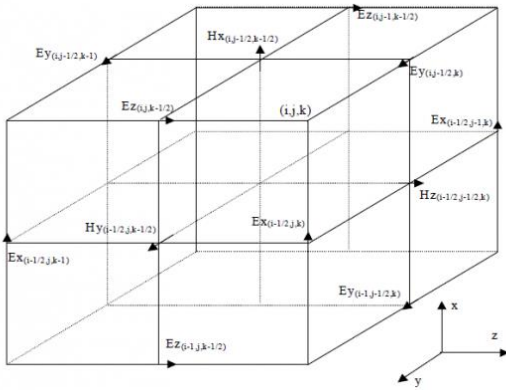


FIG. 4: A schematic representation of the displacement of the electric and magnetic field in the cubic box (Yee Space).

IV. SPR DESIGN

Our SPR study consists in analysing the reflection through the sub-wavelength holes in a gold film deposited on a crystal substrate, in our case, SiO_2 . The gold layer has a $0.2 \mu\text{m}$ of thickness and the arrays investigated consist on a square lattice with $0.6 \mu\text{m}$ of period. In the fig. 5, we show a representation in OPTIWAIVE software of our system.

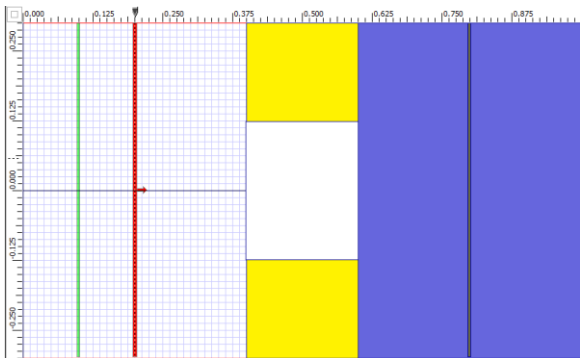


FIG. 5: The simulated design model in OPTIWAIVE designer. The yellow material corresponds to the gold, and the blue, the crystal.

We used an input plane wave modulated as a Gaussian Continuous Wave centered at $\lambda=680 \text{ nm}$ (red light). I emphasize that the dimension of the holes is larger than the

wavelength of surface plasmon waves³. Furthermore, we set up Periodic Boundary Conditions for X/Y axis to simulate a 3D infinite system of holes.

What concerns to the hole, a comparison between a cylindrical and square shapes have been studied (see FIG. 6). Our aim is to quantify the dependencies between the SPR peak and the geometry of our system, as well as the refractive index where the device is located (air, water, alcohol, etc.).

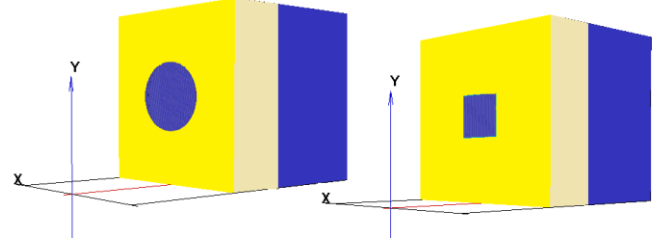


FIG. 6: Both 3D systems with cylindrical and square holes. The z-axis corresponds to the incident light propagating direction.

We have used this 2 shapes because there are 2 methods to create these arrays. For the circular holes, we could use a technique that consists on etch our substrate material (glass) with nanospheres. When the spheres have been etched (see FIG. 7 a.), the material is bombed with electrons, that will reduce their diameter, obtaining a grating as the fig 7b shows.

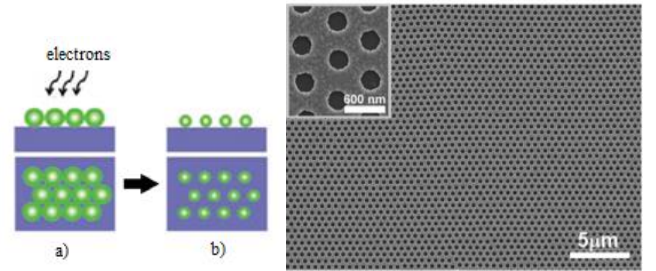


FIG. 7: Synthesized description of the first, the spheres etching and the result after the electron bombardment and the final result of the process.

Afterwards, adding a layer of gold, the metal deposit on the substrate in the places where there are not spheres. Finally, subtracting the spheres, we would get our array with the holes in the gold layer, as figure 7 shows.⁴

For the square holes, we should use Electron Beam Lithography techniques where an electron beam defines in a sensitive photoresist any pattern.⁸

V. SIMULATIONS

We consider the SPR peak as a function of the refractive index of the medium, with a period Δ of the array, a thickness L of the gold film and a characteristic dimension of the hole ϕ (the diameter for the cylinder or the side for the square) given.

$$R^{peak} = f(n; \Delta, L, \phi) \quad (3)$$

Where R^{peak} in (3) refers to the peak in the reflectance spectrum and n to the refractive index. We've focused our study on obtaining the simulated bulk sensitivity (4) of our

device against the refractive index for different environment variables for both hole shapes. In other words, figuring out how the SPR peak is shifted as a consequence of RI changes for many different configurations of our system. Thus, we would be able to know which are the dimensions and the conditions we have to build on our device to have a desired response.

$$S = \left. \frac{dR^{peak}}{dn} \right|_{\Delta, L, \phi} \quad (4)$$

A. Sensitivity with different periods

Firstly, we have done few simulations looking for the dependence between the period Δ and the reflection spectra. It could be useful if we need to design our device in a certain range of work.

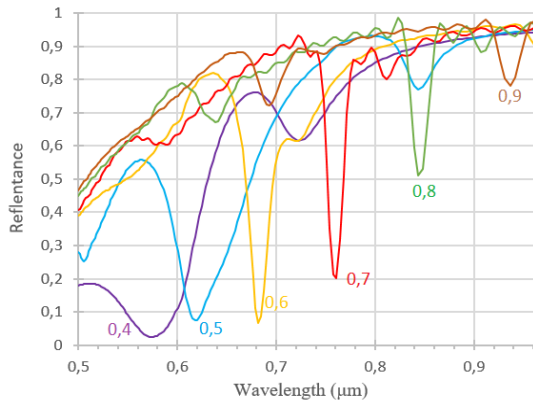


FIG. 8: Reflection curves for the array of cylindrical nanoholes with different periods (with different colours in the figure), 0.2 μm of thickness gold layer and 0.247 μm of the diameter of the hole in air ($n=1$).

Analysing the curves for the cylindrical and square shapes, we've obtained the regression for the dependence of the SPR peak versus the period (see FIG. 9).

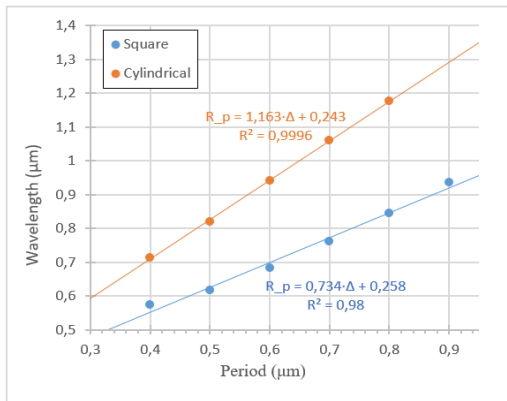


FIG. 9: Position of the peak in the reflection spectra against the period with which the device has built, in both shapes, cylindrical and square holes. For air as external medium.

A clear dependence between the period and peak is shown, even for circular and square shapes of the hole. Increasing the period results in an increase of the resonance wavelength where the SPR peak appears.

The next step is to evaluate the device sensitivity with these different periods. We will use a sample of four refractive indexes, air ($n=1$), water ($n=1.33$), Isopropanol

($n=1.38$) and Glycerol ($n=1.48$), which are the most common dielectric materials used in SPR experiments.

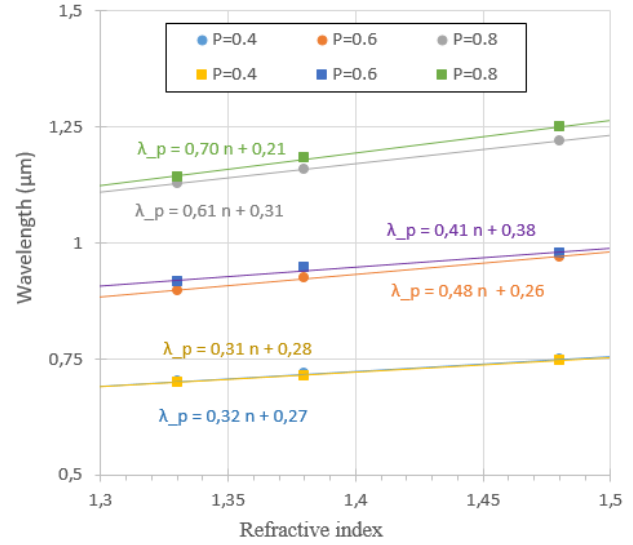


FIG. 10: Dependence between the SPR peak position with the refractive index for three different periods: 0.4, 0.6 and 0.8 μm for both shapes.

As we can observe, there is a linear dependence between the resonance wavelength and the index refraction. The sensitivity is the slope of the regressions. The larger the period, the more sensitivity we obtain.

Duty cycle	Sensitivity for the cylindrical hole	Sensitivity for the square hole
0.617	0.32	0.31
0.412	0.48	0.41
0.309	0.61	0.70

TABLE. 1: Sensitivity for both hole shapes for different duty cycles, varying the period.

B. Sensitivity with different hole size

Another important part of our simulation work has been to quantify the sensitivity using different holes. Indeed, the hole size influences the peak of the resonance, as we can see in the figure 10. For the circular area, we have considered the diameter as the size parameter, and for the square, the side.

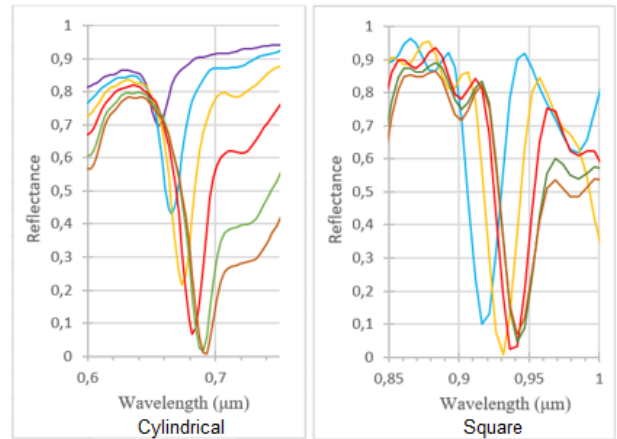


FIG. 11: Reflection spectra calculated with a gold film with 0.2 μm of thickness and a period equals to 0.6 μm , with air and a hole size as table 2 shows.

Colour	Hole size (μm)	Duty cycle
Purple	0.148	0.247
Blue	0.184	0.307
Yellow	0.213	0.355
Red	0.247	0.412
Green	0.280	0.467
Brown	0.300	0.500

TABLE. 2: Mapping of each colour with each hole size and the duty cycle (DC).

In this case, we also observe a smaller shift with the hole's size (see Fig. 11). When it comes to the square, the resonance wavelength is roughly all absorbed in the plasma, but with the cylindrical configuration we obtain a progressive absorption in the SPR peak; the bigger the hole, the bigger the absorption.

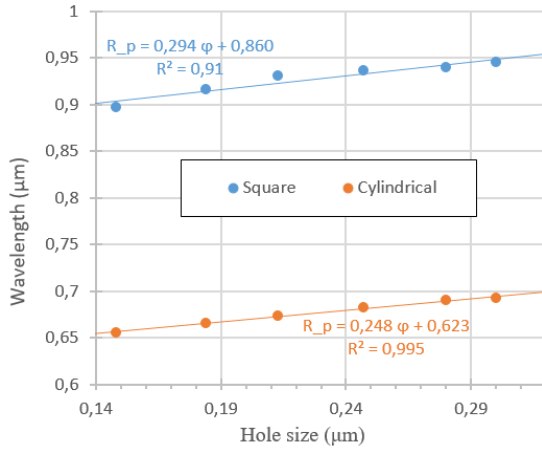


FIG. 12: SPR peak position depending on the hole's size for both types of shapes, cylindrical and square.

Furthermore, we have focused on determining the sensitivity with these different hole sizes, with the point of view on figuring out the best parameterization in order to obtain the desired SPR response. Using a $0.2 \mu\text{m}$ gold film with a $0.6 \mu\text{m}$ of period, simulations with the previous refractive indexes have been done (1.33, 1.38, 1.44).

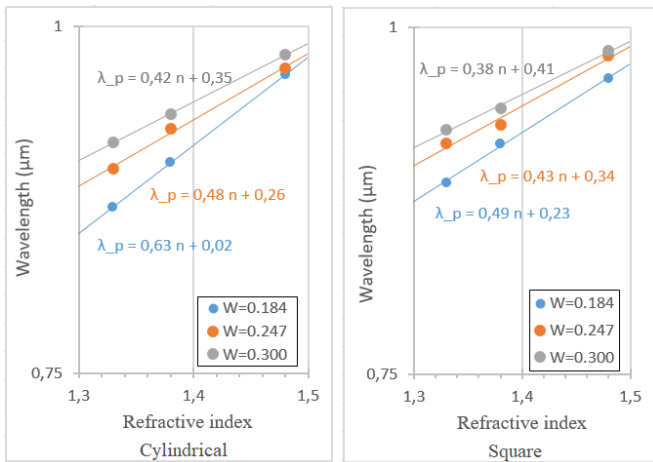


FIG. 13: SPR peak with different mediums with a configuration of a $0.2 \mu\text{m}$ gold film and a period of $0.6 \mu\text{m}$ for 3 different hole sizes: 0.184 (0.307 DC), 0.247 (0.412 DC) and 0.300 (0.5 DC) μm .

A similar response to the sensitivity with different periods is obtained, with the particularity that this time, big variations in the hole's size does not imply a really high variation in the SPR peak's position. It means that varying the hole's size, we can change the sensitivity without shifting in excess the position of the peak. In summary, increasing the duty cycle of the device, a reduction of the sensitivity appears.

C. Sensitivity with different gold film thickness

Until now, we have used a $0.2 \mu\text{m}$ thickness gold film. The next step is to quantify the relevance of this variable in the reflection spectra. Firstly, we have searched the dependence between the spectra and the thickness.

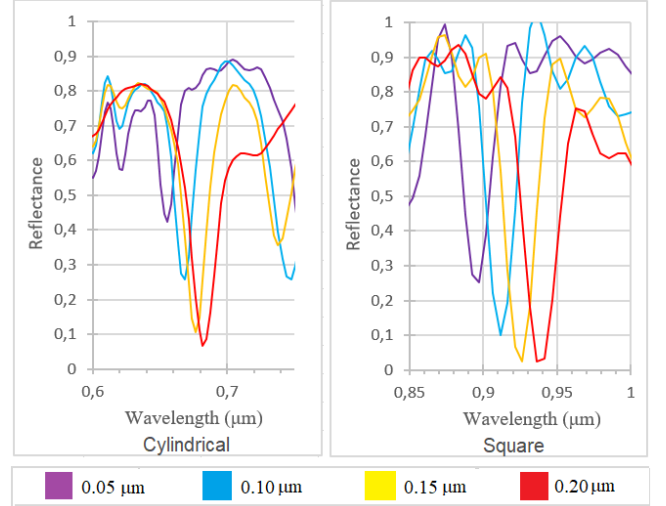


FIG. 14: Reflection spectra for the gold film with 0.412 of duty cycle and a thickness of gold film represented in different colours.

Two factors have been shown in this analysis. The thicker the gold layer, the more plasmon absorption there is. Further, an increase in the thickness entails a little shift in the SPR position as well (see FIG. 15).

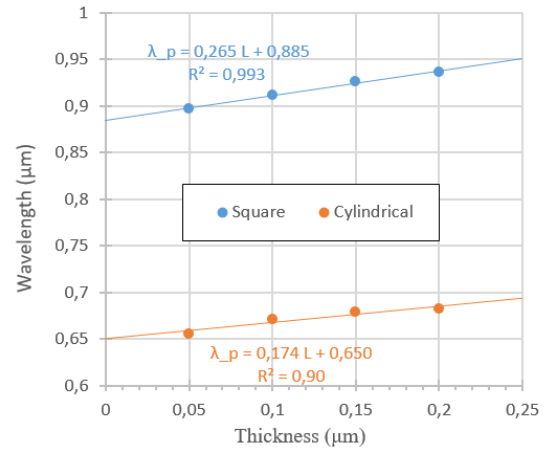


FIG. 15: Resonance peak position versus the gold film thickness corresponding to the system of the figure 13.

A similar effect to the hole size seems to provide the thickness of the layer in terms of the position of the peak in the air. Finally, we have investigated the effects in the sensitivity, as we did for the other parameters.

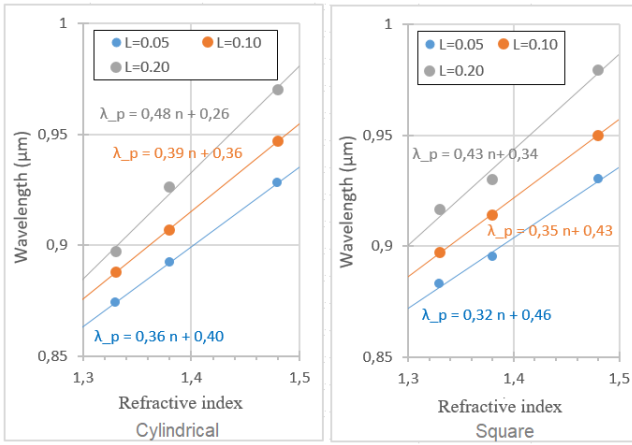


FIG. 16: SPR peak with different mediums with a configuration of a 0.247 hole's size and a period of 0.6 μm (0.412 DC) for 3 different gold layer thickness: 0.05, 0.10 and 0.20 μm .

VI. CONCLUSIONS

We have shown that OPTIWAVE is a really useful software for carrying out SPR simulations, and it offers the possibility to pre calculate and pre design the parameters of your SPR device based on a gold-thin-film with 3D nanoholes. After this study, we can say the following:

- Working with visible light, increasing the period, the hole's size, or the thickness of the gold in the SPR device, shifts the SPR peak to the infrared wavelengths (longer wavelength).
- Increasing the period suppose an augment of the sensitivity of the device.
- On the other hand, the bigger the hole, the less sensitivity the device has.
- Resemblance effect for the lattice period is shown with the gold thickness. As thick is the layer, more sensitivity it has.
- Both hole's shapes studios haven't implied big changes to the sensitivity, and the behaviour is similar.

- In terms of the actual spectrometers precision, these shifts in the SPR peak can be detected easily when it comes to biosensors framework, detecting small changes in the refractive index.
- What concerns to the loss of the incident light and the absorption in the resonance wavelength, useful optical light filters can be built, without losing the major part of the intensity, and removing the desired wavelength.

VII. APPENDIX

I would like to give what were the simulation parameters I've used in this work on Optiwave Designer. For the FDTD method we have:

Mesh Delta X: 0.005 μm with 120 cell;
Mesh Delta Y: 0.005 μm with 120 cell;
Mesh Delta Z: 0.005 μm with 200 cell;
 1200 time steps

And for the Spectral DFT Simulation parameters:

Number of samples: 200
Start wavelength: 0.5 μm
End wavelength: 1.2 μm

The time expended in a computer with Intel Core 2 Duo E7500 processor was for roughly 2 hours for each reflection spectra. 86 spectrums were simulated.

Acknowledgments

Firstly, I would like to thank to Mauricio Moreno for all the knowledge given to me, introducing myself to the more applied physics, letting me use the OPTIWAVE software in the university.

I would like to thank to Miquel Duart and Andreu Benavent for the support while we were sharing the software as well.

Finally, I greatly appreciate the support received from my family that was a very good motivation to move forward in this work.

-
- [1] Research Gate, article «Kretschmann configuration» [online]: <https://www.researchgate.net/>
- [2] SariSabban - Sabban, Sari (2011) «Development of an in vitro model system for studying the interaction of Equus caballus IgE with its high-affinity FcεRI receptor» (PhD thesis), The University of Sheffield
- [3] Optiwave documentation [online]: <http://optiwave.com/>
- [4] Si Hoon Lee et al, «Self-Assembled Plasmonic Nanohole Arrays», 1975.
- [5] Lauren E. Kreno et al, «Metal-Organic Framework Thin Film for Enhanced Localized Surface Plasmon Resonance Gas Sensing», 2010.
- [6] Xiangxian Wang et al, «Theoretical Investigation of a Highly Sensitive Refractive-Index Sensor Based on TM0 Waveguide Mode Resonance Excited in an Asymmetric Metal-Cladding Dielectric Waveguide Structure », 1975.
- [7] Qin Chen et al, «Nanophotonic Image Sensors».
- [8] Hakan Inan et al, «Photonic crystals: emerging biosensors and their promise for point-of-care applications».

